available at www.sciencedirect.com

www.elsevier.com/locate/matchar

Mechanism of SiC crystals growth on {100} and {111} diamond surfaces upon microwave heating

P. Unifantowicz[a,b,*], S. Vaucher[b], M. Lewandowska[a], K.J. Kurzydłowski[a]

[a] The Faulty of Materials Science and Engineering, Warsaw University of Technology, Wołoska 141, 02-507 Warsaw, Poland
[b] EMPA—Swiss Federal Laboratories for Materials Testing and Research, Department of Materials Technology, Feuerwerkerstrasse 39, 3604 Thun, Switzerland

ARTICLE DATA

Article history:
Received 20 May 2009
Received in revised form
11 February 2010
Accepted 24 March 2010

Keywords:
Diamond
SiC
Microwave sintering
TEM

ABSTRACT

The subject of this work is focused on characterization of the microstructures and orientations of SiC crystals synthesized in diamond–SiC–Si composites using reactive microwave sintering. The SiC crystals grown on the surfaces of diamonds have either shapes of cubes or hexagonal prisms, dependent on crystallographic orientation of diamond. The selection of a specified plane in diamond lattice for the TEM investigations enabled a direct comparison of SiC orientations against two types of diamond facets. On the {111} diamond faces a 200 nm layer of 30–80 nm flat β-SiC grains was found having a semi-coherent interface with diamond at an orientation: (111)[112]SiC‖(111)[110]C. On the {100} diamond faces β-SiC forms a 300 nm intermediate layer of 20–80 nm grains and an outer 1.2 μm layer on top of it. Surprisingly, the SiC lattice of the outer layer is aligned with the diamond lattice: (111)[110]SiC‖(111)[110]C.

1. Introduction

Diamond–SiC composites are considered one of the most promising materials for thermal management applications. In contrast with metal-based diamond composites, diamond–SiC potentially combine high thermal conductivity and relatively low coefficient of thermal expansion of two phases each having a low density.

Chemical bonding between the diamond particles and the SiC should be provided by a reaction between carbon and silicon to form 'bridges' structurally integrated with diamond. However, the thermal resistance of SiC–diamond interfaces should be minimised to ensure efficient heat transport in the interconnected diamonds [1,2]. This can be achieved by providing defect-free, coherent interfaces between the diamond and the SiC lattices. It should be noted that the SiC crystals can grow on diamond either in an ordered fashion, resulting in highly strained epitaxial layers, low energy semi-coherent configurations [3,4] or through high-misfit interfaces with lattice defects minimizing the strain energy [5]. Numerous investigations have been carried out on the structure of SiC–diamond interfaces [5–9]. However, to the best knowledge of the authors, the growth mechanism of SiC crystals grown on differently oriented diamond surfaces has not been studied and experimentally verified.

The diamond–SiC composites can be fabricated via high-temperature high-pressure sintering of diamond and Si [6–9], infiltration of diamond compacts with precursor gas [10] and more recently by microwave reactive sintering of diamond–silicon powders mixtures [11,12]. In contrast to the conventional processes, microwave sintering has the advantage of internal and phase-selective heat generation which offers high sintering rates [13]. Since silicon has a much higher dielectric loss than diamond, it more readily absorbs microwave energy and is preferentially heated to temperatures above its melting point [14]. The higher heating rate facilitated

* *Corresponding author*. EMPA—Swiss Federal Laboratories for Materials Testing and Research, Department of Materials Technology, Feuerwerkerstrasse 39, 3604 Thun, Switzerland. Tel.: +41 563102957; fax: +41 563104529.
E-mail address: Paulina.Unifantowicz@psi.ch (P. Unifantowicz).

1044-5803/$ – see front matter © 2010 Elsevier Inc. All rights reserved.
doi:10.1016/j.matchar.2010.03.010

by the use of microwaves reduces the sintering time which helps avoid overheating of the diamond particles, thereby preventing their graphitization.

Electron microscopy (SEM and TEM) was used to characterize the morphology and crystallographic relations between the SiC and diamond crystals. The obtained results elucidated the mechanism of SiC growth on differently oriented planes of diamond in microwave sintered diamond–SiC composites.

2. Experimental

Diamond MBD8 monocrystals (Qiming) having an average diameter of 150 μm and n-doped Si powder with particle diameter of about 0.22 μm obtained by milling Czochralski monocrystal were used for sintering. The powders were mixed at Si:diamond weight ratio of 1:4 in Turbula mixer and heated at 90 °C/min up to 1700 °C under argon using microwaves (2.45 GHz, 1 kW max., Dipolar AB, TE103 resonator, Raytek pyrometer). The general structure of the as-sintered samples was investigated using scanning electron microscope (Hitachi S-3500N). The microstructures of the SiC–diamond interfaces were revealed by transmission electron microscopy (JEOL JEM 1200) and the TEM foils were prepared using focused ion beam technique (Hitachi FB2100). The microstructures of SiC layers were examined using bright field TEM images while the structure and crystallographic orientations of the SiC crystals were revealed using selected area electron diffraction patterns.

3. Results

Microwave sintering allowed synthesis of mechanically stable, porous compacts of interconnected diamonds. The open porosity of the as-sintered samples measured by pycnometer and Archimedes method was of about 44 vol.% and closed porosity of about 2 vol.%. Although the pores bring no contribution to the macroscopic thermal conductivity, the porous structure of the composite enables the investigation on morphology and distribution of the compounds grown on the surfaces of diamonds.

The X-ray powder diffraction patterns of the pulverised samples revealed characteristic peaks of diamond, cubic Si and cubic β-SiC, Fig. 1. Since the β-SiC polytype and diamond have the cubic zinc blende structure, their lattices tend to have a crystallographic alignment which should provide efficient phonon transport through the interfaces.

The SEM analysis of the diamond–SiC–Si composite samples showed that the diamonds were bonded into porous pre-forms by 'bridges' made of silicon carbide and remnant silicon, Fig. 2. The presence of SiC layers at the interfaces between diamonds and solidified silicon droplets indicated good wetting of the diamond surfaces by molten Si. Cubic SiC crystals were found on the square diamond facets having {100} orientation while flat, hexagonal SiC prisms were observed on the hexagonal {111}-oriented facets.

The microstructures of the SiC layers developed on the {100} and {111}-oriented diamond facets were revealed by cross-sectioning the respective diamond surfaces along <110> directions using FIB, as illustrated in Fig. 3. For SiC lattice matching that of diamond, the selection of the {110} plane view in the cubic or {11–20} in hexagonal SiC crystal allows a straightforward identification of the SiC polytype, as explained in [3]. The schematic in Fig. 3 shows that the morphology of SiC crystals reflects the geometry of the specific diamond facet, as indicated by the SEM micrographs. The so-called periodic bond chain theory implies that the bond structure of the substrate surface determines the growth habit and the morphology of the new crystal [15].

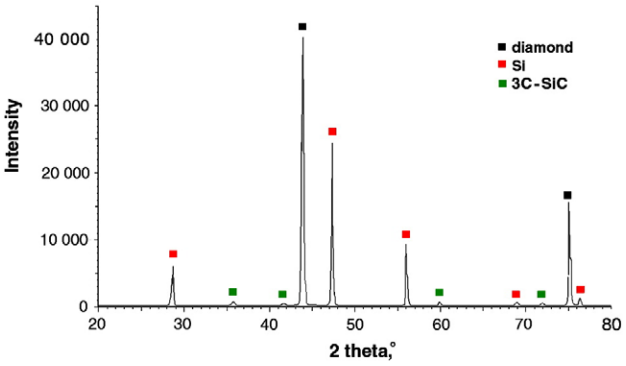

Fig. 1 – XRD spectrum of the as-sintered diamond–SiC–Si composite.

The TEM micrographs of the SiC crystals grown on a {100}-oriented diamond surface revealed a two-layer microstructure, Fig. 4 (a). A dense, about 1.2 μm thick layer of SiC crystals is separated from diamond by a 300 nm layer consisting of equiaxed SiC grains with an average diameter of 80 nm. The bright field TEM images showed irregular stacking faults along the {111} planes in the microcrystalline SiC layer. The formation energy for these stacking faults in β-SiC is very low (1.9 mJ/m^2) [16] thus they can easily be formed under thermal stresses during sintering. Steps were observed at the SiC–diamond interface, suggesting local etching and roughening of diamond {100} surface. As a result, the {111} facets of diamond were revealed, as indicated by the inclination angle of about 70° between the steps, the same as between the (111)

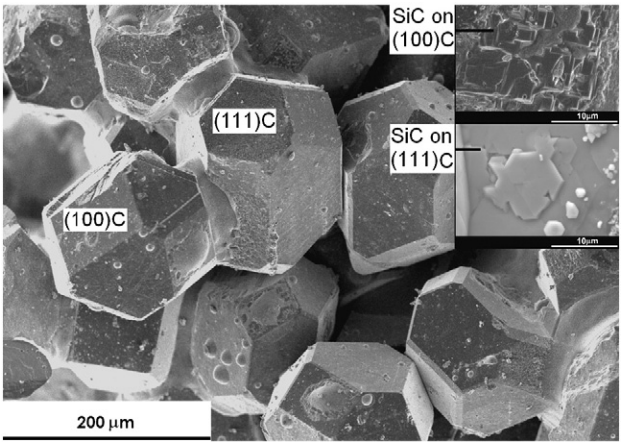

Fig. 2 – SEM micrograph of the as-sintered diamond–SiC–Si composite; inclusions show the top-view of the SiC crystals on the {100} and {111} diamond facets.

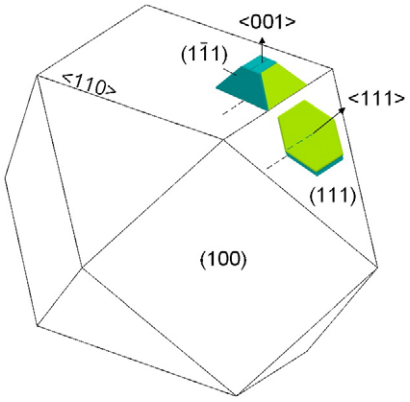

Fig. 3 – A schematic showing the morphology of the SiC crystals grown on two types of diamond facets with the selected section lines.

and (−1–1 1) planes in a cubic lattice. The steps on the {100} facets are most likely related to enhanced reactivity of these surfaces due to a two time higher density of unpaired bonds compared with the less reactive {111} facets. The SiC crystals found on the {111}-oriented diamond facets make up a more uniform layer, with thickness of about 200 nm, consisting of flat grains with thickness in the range of 30–80 nm, Fig. 4 (b). This layer is significantly thinner than the one developed on the {100}-oriented diamond, which indicates lower reactivity of hexagonal diamond facets.

The EDX line scans through the SiC–diamond interface for the {100} and {111}-oriented diamond are shown in Fig. 4 (c) and (d), respectively. A decrease of Si atoms concentration in the outer, microcrystalline SiC layer could be due to bulk diffusion of Si atoms toward the SiC–diamond interface. The profiles of C and Si concentrations in the intermediate nano-layer on the {100} diamond might indicate its non-stoichiometric composition. However, due to a limited accuracy of the measurement this result might be an artifact and should be supported by other investigation methods.

The formation of β-SiC polytype on both types of diamond facets was confirmed by the selected area electron diffraction. The analyses of the SAED patterns for SiC crystals on the {100} diamond surface revealed identical orientation with diamond, that is: (111)[110]SiC‖(111)[110]C, Fig. 5 (a). However, the presence of the intermediate layer with randomly oriented SiC nano-grains, Fig. 5 (b), rules out epitaxy of the upper microcrystalline SiC layer. In the case of the {111} diamond face, the following orientation relation between SiC and diamond was found from the SAED pattern: (111)[112] SiC‖(111)[110]C, Fig. 5 (c), indicating a semi-coherent interface. For this orientation, the SiC lattice is rotated by 30° around [111] axis with respect to diamond lattice. This situation has been shown on a model of coincident lattice sites in the diamond–SiC interface given in [5]. In the case of β-SiC–diamond interfaces, a match with low index planes, such as {100} is more likely than with the higher index planes, such as {112}, {114} and {221}; however, the latter are energetically favourable [4]. Considering a relatively large difference in the lattice parameter of SiC and diamond (~18%), the SiC lattice is unlikely to deform to maintain an epitaxial relation. Therefore, the generation of semi-coherent interfaces, providing coincident lattice sites, reduces the mismatch and the related strains at the diamond–SiC interface.

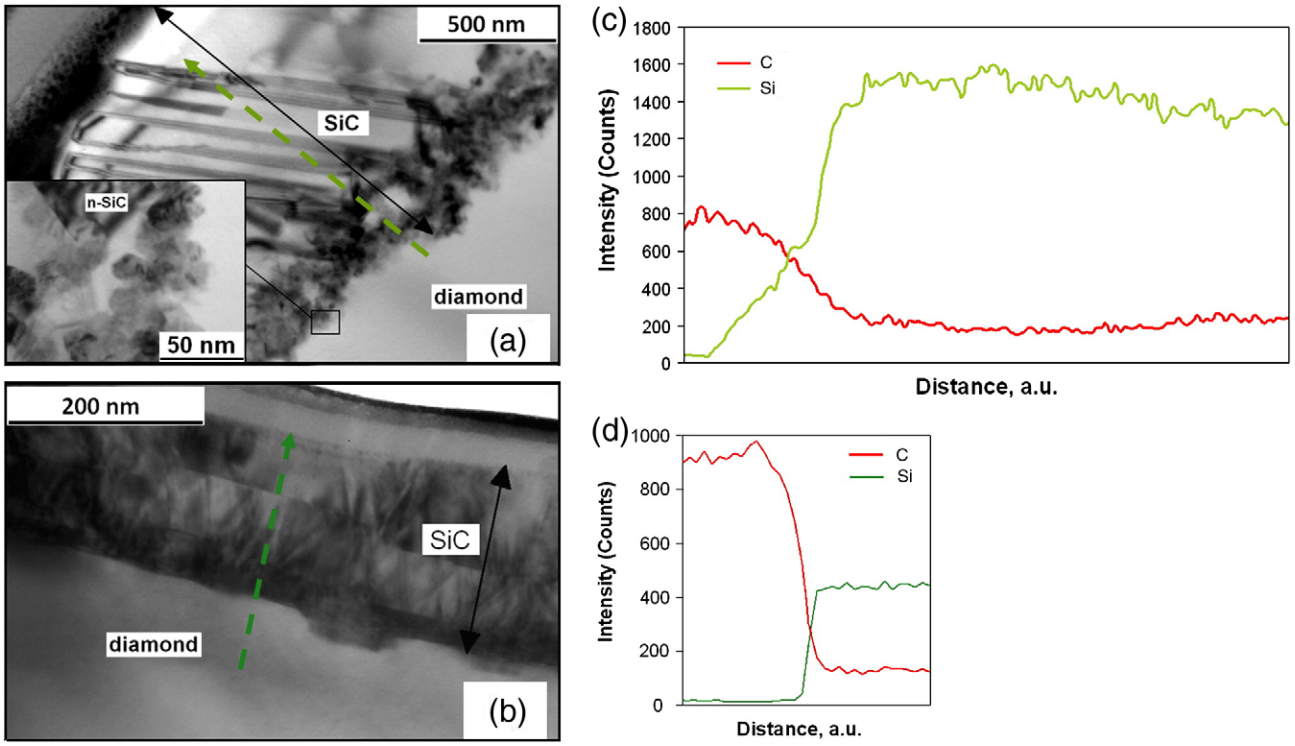

Fig. 4 – Bright field TEM images of the interfacial SiC layers on (a) {100} and (b) {111} diamond with EDX line scans of SiC layers on (c) {100} (d) {111} diamond.

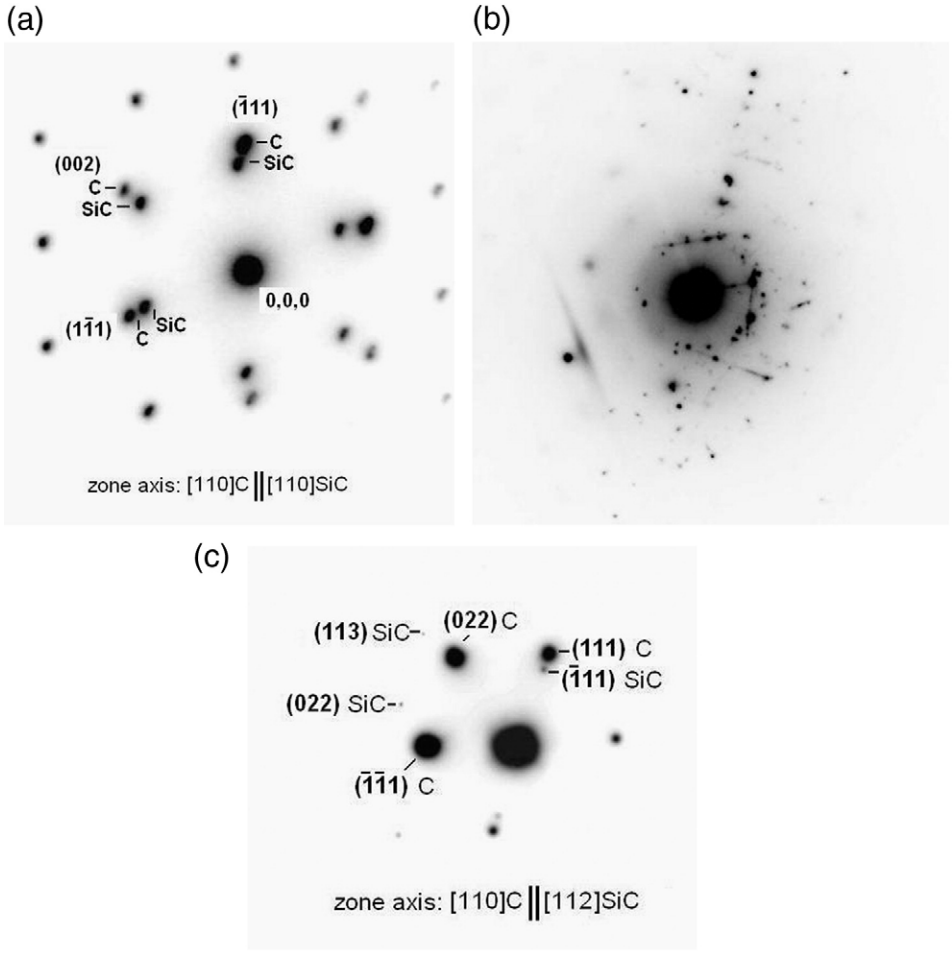

Fig. 5 – SAED patterns of the interfacial areas: (a) microcrystalline SiC and {100}-oriented diamond, (b) nano-crystaline SiC sub-layer grown on the same diamond and (c) SiC crystals and {111}-oriented diamond.

The microscopic observations allowed describing the growth mechanism of SiC crystals on {111} and {100} diamond facets in the diamond–SiC–Si composites. The SiC crystals expand much faster in directions parallel to the {111} planes than in perpendicular direction because the {111} surfaces have the densest atom stacking and the lowest surface energy. Formation of flat SiC crystals by development of the {111} planes on the {111} diamond facets is therefore favoured. In the case of the {100} diamond facets, due to surface roughening numerous etch pits serve as nucleation sites for SiC crystals. The walls of these etch pits having {111} orientations are inclined towards the {100} surface of diamond. The {111} SiC planes grow preferentially on the diamond planes of the same orientation along the etched walls. In this case the planes of the fastest growth are inclined to the diamond surface, thus the SiC crystal growth on {100} diamond prevails in the direction perpendicular to its surface.

The following mechanism leading to formation of the double SiC layer was proposed based on the TEM and SAED. The first SiC crystals precipitate at the interface between diamond and liquid Si from the saturated $Si_L(C)$ solution. When the primary SiC crystals form a dense layer, the diamond substrate is shielded from the silicon and thus the transport of the reagents slows down. Then, the SiC layer grows mainly outwardly by saturation of the Si melt with the C atoms diffusing through the SiC layer. Simultaneous diffusion of Si atoms in the opposite direction, toward the diamond results in precipitation of SiC crystals at the interface between the diamond and the primary SiC crystals.

4. Conclusions

The microscopic observations showed that the differences in the crystallographic orientation and roughness of diamond {111} and {100} surfaces determine the orientation, morphology and thickness of SiC crystals growing on them. Three-dimensional growth of SiC crystals on the {100} diamond involves creation of numerous steps on its surface in contrast with the {111} diamond on which the SiC crystals grow in a two-dimensional manner. The SiC cubes and thin hexagonal prisms were found on the {100} and {111} facets, respectively. On the {100} diamond, SiC micro-grains are in crystallographic alignment with the diamond and are separated from it by randomly oriented nano-grains. On the {111} diamond, SiC

crystals create a semi-coherent interface with mutual rotation of the two lattices by the [111] axis. According to the proposed growth mechanism, the separation of the diamond from liquid Si by the primary SiC crystals leads to the formation of a secondary layer made of SiC nano-crystals. The presence of the intermediate layer of randomly oriented nano-grains is expected to decrease the thermal transport properties of the diamond–SiC composites.

Acknowledgements

This work was carried out in the frame of the International PhD School Switzerland–Poland. The authors acknowledge Dr. Jerzy Morgiel and Dr. Justyna Grzonka from the Institute of Metallurgy and Materials Science of the Polish Academy of Sciences, Kraków for help with the TEM analysis.

REFERENCES

[1] Hasselman D, Johnson L. Effective thermal conductivity of composites with interfacial thermal barrier resistance. J Comp Mater 1987;21:508–15.
[2] Jagannadham K, Wang H. Thermal resistance of interfaces in AlN–diamond thin film composites. J Appl Phys 2002;91: 1224–35.
[3] Kusumori T, Muto H, Brito ME. Control of polytype formation in silicon carbide heteroepitaxial films by pulsed-laser deposition. Appl Phys Lett 2004;84:1272–4.
[4] Zhu W, Wang XH, Stoner BR, Kong HS, Braun MWH, Glass JT. Geometric modeling of the diamond–β-SiC heteroepitaxial interface. Diamond Relat Mater 1993;2:590–6.
[5] Park JS, Sinclair R, Rowcliffe D, Stern M, Davidson H. Orientation relationship in diamond and silicon carbide composites. Diamond Relat Mater 2007;16:562–5.
[6] Pantea C, Voronin GA, Zerda TW, Zhang J, Wang L, Wang Y, et al. Kinetics of SiC formation during high P–T reaction between diamond and silicon. Diamond Relat Mater 2005;14: 1611–5.
[7] Pantea C, Voronin GA, Zerda TW. Kinetics of the reaction between diamond and silicon at high pressure and temperature. J Appl Phys 2005;98:073512-5p.
[8] Voronin GA, Zerda TW, Qian J, Zhao Y, He D, Dub SN. Diamond–SiC nanocomposites sintered from a mixture of diamond and silicon nanopowders. Diamond Relat Mater 2003;12:1477–81.
[9] Ekimov EA, Gromnitskaya EL, Mazalov DA, Pal AF, Pichugin VV, Gierlotka S, et al. Microstructure and mechanical characteristics of nanodiamond–SiC compacts. J Phys Solid State 2004;46:755–7.
[10] Lee J-H, Benzel JF, Lackey WJ. In: Wachtman Jr JB, editor. Advanced ceramics, materials, and structures—B: Ceramic Engineering and Science Proceedings, 16; 2008. p. 1145–50.
[11] Leparoux S, Diot C, Dubach A, Vaucher S. Synthesis of silicon carbide coating on diamond by microwave heating of diamond and silicon powder: a heteroepitaxial growth. Scr Mater 2007;57:595–7.
[12] Vaucher S, Unifantowicz P, Ricard C, Dubois L, Kuball M, Catala-Civera J-M, et al. On-line tools for microscopic and macroscopic monitoring of microwave processing. Phys B: Condensed Matter 2007;398:191–5.
[13] Samuels J, Brandon JR. Effect of composition on the enhanced microwave sintering of alumina-based ceramic composites. J Mater Sci 1992;27:3259–65.
[14] Vaucher S, Catala-Civera J-M, Sarua A, Pomeroy J, Kuball M. Phase selectivity of microwave heating evidenced by Raman spectroscopy. J Appl Phys 2006;99:113505 [5 pp.].
[15] Sun B, Zhang X, Lin Z. Growth mechanism and the order of appearance of diamond (111) and (100) facets. Phys Rev B 1993;47:9816–24.
[16] Stevens R. Defects in silicon carbide. J Mater Sci 1972;7:517–21.